Environmental Science & Technology

pubs.acs.org/est

Article

Effect of Metal Ions on Oxidation of Micropollutants by Ferrate(VI): Enhancing Role of Fe^{IV} Species

Xianbing Zhang,[⊥] Mingbao Feng,[⊥] Cong Luo, Nasri Nesnas, Ching-Hua Huang,* and Virender K. Sharma*

Cite This: *Environ. Sci. Technol.* 2021, 55, 623−633

Read Online

ACCESS | Metrics & More | Article Recommendations | Supporting Information

ABSTRACT: This paper investigated the oxidation of recalcitrant micropollutants [i.e., atenolol (ATL), flumequine, aspartame, and diatrizoic acid] by combining ferrate(VI) ($Fe^{VI}O_4^{2-}$, Fe^{VI}) with a series of metal ions [i.e., Fe(III), Ca(II), Al(III), Sc(III), Co(II), and Ni(II)]. An addition of Fe(III) to Fe^{VI} enhanced the oxidation of micropollutants compared solely to Fe^{VI}. The enhanced oxidation of studied micropollutants increased with increasing [Fe(III)]/[Fe^{VI}] to 2.0. The complete conversion of phenyl methyl sulfoxide (PMSO), as a probe agent, to phenyl methyl sulfone ($PMSO_2$) by the Fe^{VI}−Fe(III) system suggested that the highly reactive intermediate Fe^{IV}/Fe^{V} species causes the increased oxidation of all four micropollutants. A kinetic modeling of the oxidation of ATL demonstrated that the major species causing the increase in ATL removal was Fe^{IV}, which had an estimated rate constant as $(6.3 \pm 0.2) \times 10^4\ M^{-1}\ s^{-1}$, much higher than that of Fe^{VI} [$(5.0 \pm 0.4) \times 10^{-1}\ M^{-1}\ s^{-1}$]. Mechanisms of the formed oxidation products of ATL by Fe^{IV}, which included aromatic and/or benzylic oxidation, are delineated. The presence of natural organic matter significantly inhibited the removal of four pollutants by the Fe^{VI}−Fe(III) system. The enhanced effect of the Fe^{VI}−Fe(III) system was also seen in the oxidation of the micropollutants in river water and lake water.

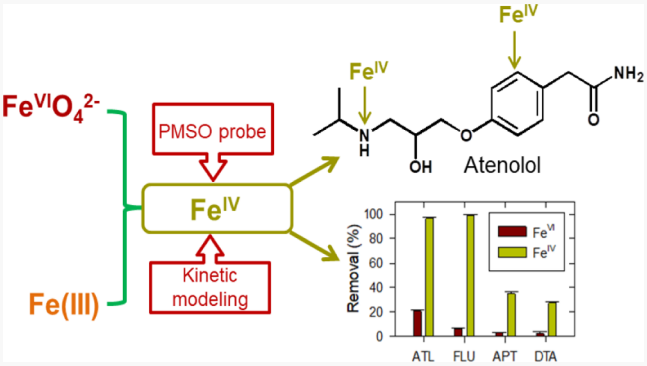

INTRODUCTION

In the past decade, the concerns with water pollution have intensified because of an increase in consumer demand for better water quality. Micropollutants like pharmaceuticals, hormones, and personal care products are generally present in water and are potentially toxic to human health and ecosystems.[1] These micropollutants are indispensable in society, resulting in an increase in their production to several hundred million tons per year.[2] Researchers continue to develop new technologies to treat micropollutants in water that can be classified as biological, adsorption, membrane, and advanced oxidation processes.[3−7] Biological treatments usually do not have the oxidizing ability to eliminate micropollutants. Adsorption and membrane processes are physicochemical methods that only transfer micropollutants from one phase to another without degrading them. Among oxidative processes, the use of iron has been regularly proposed to remediate micropollutants. Iron is one of the most abundant metals on earth and its application in treating micropollutants is attractive. The processes of iron-based materials with oxidation states ranging from 0 to +6 have been shown to eliminate micropollutants. This includes zero-valent iron [Fe(0)] technology, Fenton and Fenton-like reactions [e.g., Fe(II)/Fe(III)−H_2O_2], and ferrate(VI) ($Fe^{VI}O_4^{2-}$ or Fe^{VI}) oxidations.[8−12]

In recent years, research on the applications of Fe^{VI} has been increasing because of its potential in multifunctional water treatment like coagulation, oxidation, and disinfection.[13−19] Many investigations using Fe^{VI} have been carried out to oxidize micropollutants.[20−22] Fe^{VI} could oxidize most of the micropollutants at significant rates, but other compounds of interest have shown sluggish reactivity with Fe^{VI} resulting in a much less effective removal.[23] Recent efforts are in progress to activate Fe^{VI} to enhance elimination of recalcitrant micropollutants in water.[17,24,25] In our laboratory, we have used reducing anions in combination with Fe^{VI} to effectively oxidize pollutants in water.[24] The current paper explores the combinations of Fe^{VI}−metal ions to increase the oxidizing ability of Fe^{VI} with an objective to uncover environmental-

Received: July 14, 2020
Revised: November 21, 2020
Accepted: December 2, 2020
Published: December 16, 2020

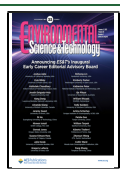

friendly metal ions that achieve efficient oxidation of a wide range of micropollutants.

Limited work has been performed to see the effects of metal ions on oxidation of pollutants by Fe^{VI}. The metal ions studied were only Fe(III), Fe(II), and Mn(II) for water remediation [e.g., removal of diclofenac (DCF)] by Fe^{VI} in water without buffering.[26−28] An increased removal of DCF was seen when these metal ions were present in a mixed solution of Fe^{VI}−DCF. However, a later study using Fe(III) in borate buffer solution at pH 8.0 found no influence on the oxidation of DCF and the suggestion was made that the observed increase in oxidation of DCF in former studies was because of decrease in pH as a result of adding Fe(III) solution into the mixed aqueous solution of Fe^{VI}−DCF.[29] Fe^{VI} has shown an increase in oxidation power with a decrease in pH.[11] Additionally, a recent study using borate buffer at pH 8.0 reported a higher removal of sulfamethoxazole (SMX) by the Fe^{VI}−Fe(III) system than only Fe^{VI}.[13] This study hypothesized the enhanced formation of Fe^{V} and Fe^{IV} by Fe(III)-catalyzed degradation of Fe^{VI}. The discrepancies in the observed effects of Fe(III) on the oxidation of the pollutants by Fe^{VI} intrigued us to examine the influence of metal ions on the oxidation of pollutants by Fe^{VI}.

The present paper studied different metal ions [i.e., Fe(III), Ca(II), Al(III), Sc(III), Co(II), and Ni(II)] to learn if the type of metal ions has any role in oxidizing pollutants by Fe^{VI}. Salts of Fe(III) and Al(III) are commonly used as coagulants and may accelerate the formation of intermediate high-valent iron species from Fe^{VI}. The particles of Fe(III) have shown to increase the decomposition of Fe^{VI}.[30,31] Another study has also shown that Ca(II) could enhance the decomposition of Fe^{VI} by water under alkaline conditions.[32] The role of redox-inactive metal ions [i.e., Ca(II) and Sc(III)] has been investigated in biomimetic oxidation reactions in nonaqueous environment, which showed that these metal ions modulated the reactivity of high-valent iron complexes with increase in oxidizing ability and alternation of mechanism because of the varied coordination environments around the central iron atom.[33−35] No information of such redox-inactive metal ions on the oxidation power of high-valent iron-oxo species like Fe^{VI} under aqueous environment is currently known. Trace amounts of transition metal ions, such as Co(II) and Ni(II), could rapidly decompose Fe^{VI} in water,[36] which may produce large amounts of Fe^{IV}/Fe^{V} species in a short time, before being converted to Fe(III) leading to an acceleration of oxidations by Fe^{VI}. Formation of Fe^{IV}/Fe^{V} species has been seen in thermal decomposition of solid salts of Fe^{VI} at 235 °C,[37,38] and formation of such iron intermediates may also occur under aqueous solution and room-temperature conditions. Furthermore, once the Fe^{IV}/Fe^{V} species are formed, their structures and properties would vary with the cations (or metal ions) present in solution-like synthesized salts of Fe^{VI} having different metal ions.[39−41] The current study thus investigated for the first time the varying systems of enhanced oxidation of Fe^{VI} in combination with different metal ions. We also explored whether a Fe(III)−TAML (TAML = tetra-amide macrocyclic ligand) complex enhances the oxidation of pollutants by Fe^{VI} because of the anticipated formation of Fe^{IV}/Fe^{V} species, as previously observed in systems of Fe(III)−TAML with H_2O_2 and hypochlorite, which have shown high ability to oxidize micropollutants.[42,43]

In this work, we first added Fe(III) to Fe^{VI} to oxidize four micropollutants [i.e., atenolol (ATL), flumequine (FLU), aspartame (APT), and diatrizoic acid (DTA)], followed by studying other metal ion additions to the Fe^{VI}-contaminant solution. These micropollutants have varied structures and have shown sluggish reactivity with Fe^{VI} (Table S1). The molecules of these micropollutants possess moieties resilient toward oxidation such as an amide-isopropylamino alcohol, a vinylogous amide/acid, a dipeptide ester, and a bulky triiodoaromatic amide/acid, respectively. Fe^{VI} shows low reactivity with such moieties in molecules.[20,44] Oxidation experiments using different Fe^{VI}−metal ions could establish the role of each type of metal ion in any potential increase in the removal of the pollutant. Products of the oxidation of phenyl methyl sulfoxide (PMSO) by Fe^{VI}−Fe(III) showed the participation of Fe^{V}/Fe^{IV} species.[13] A kinetic modeling of the degradation of the micropollutant was applied to clearly demonstrate that Fe^{IV} species was the dominant oxidant enhancing the oxidation ability of the Fe^{VI}−Fe(III) system. Oxidized products (OPs) of ATL in the Fe^{VI}−Fe(III) system were identified, and the proposed mechanisms of their formation in the presence of Fe^{IV} were elucidated. The relevance of the Fe^{VI}−Fe(III) system in treatment processes was explored by studying the influence of ions (e.g., carbonate and phosphate), pH, and natural organic matter (NOM) on pollutant removal. Finally, removal of the pollutants in surface water samples (i.e., lake water and river water) was examined in the Fe^{VI}−Fe(III) system.

■ EXPERIMENTAL SECTION

Chemicals and Reagents. Detailed information on the target micropollutants (i.e., ATL, FLU, APT, and DTA), Fe^{VI} solutions, preparation of all metal ions and other reaction solutions, and physicochemical characteristics of surface water samples is given in Text S1.

Removal Experiments. The removal experiments of micropollutants by Fe^{VI}−metal ion systems were conducted in triplicates in 100 mL beakers under a constant stirring rate of 400 rpm at room temperature. The reactions of micropollutants (5.0 μM) and Fe^{VI} (100.0 μM) with and without the addition of Fe(III) (0−200.0 μM) were initiated by mixing equal solution volumes of 10.0 mL, and the reaction mixtures were maintained at pH 9.0 using 2.0 mM borate buffer. The reaction solutions were quenched at certain reaction times (i.e., 0−20 min) completely using 20.0 μL of 1.0 M hydroxylamine solution. Samples were filtered using 0.45 μm polytetrafluoroethylene syringe filters (Fisherbrand, Fisher Scientific) and transferred into 2.0 mL high-performance liquid chromatography (HPLC) vials for analysis. Additionally, six representative metal ions/complex (i.e., Fe^{III}−TAML, Fe(III), Ca(II), Al(III), Sc(III), Co(II), and Ni(II)) were also individually added into Fe^{VI}−ATL solutions to learn their effect on ATL removal. To better evaluate the remediation performance of the Fe^{VI}/Fe(III) system for practical applications, 5−20 mg/L of two typical NOM [i.e., Suwannee River humic acid (SRHA, 52.63% C) and Suwannee River NOM (SRNOM, 50.70% C)], which were obtained from International Humic Substances Society (St. Paul, MN), and carbonate and phosphate at 5.0 mM were individually preadded to study their possible effects. Details of removal experiments of DTA in surface water samples are provided in Text S2.

Analytical Procedures. The concentration changes of target micropollutants during Fe^{VI}−metal ion oxidations were monitored using an Ultimate 3000 ultrahigh-performance liquid chromatography (Thermo Fisher Scientific) with a UV

https://dx.doi.org/10.1021/acs.est.0c04674
Environ. Sci. Technol. 2021, 55, 623−633

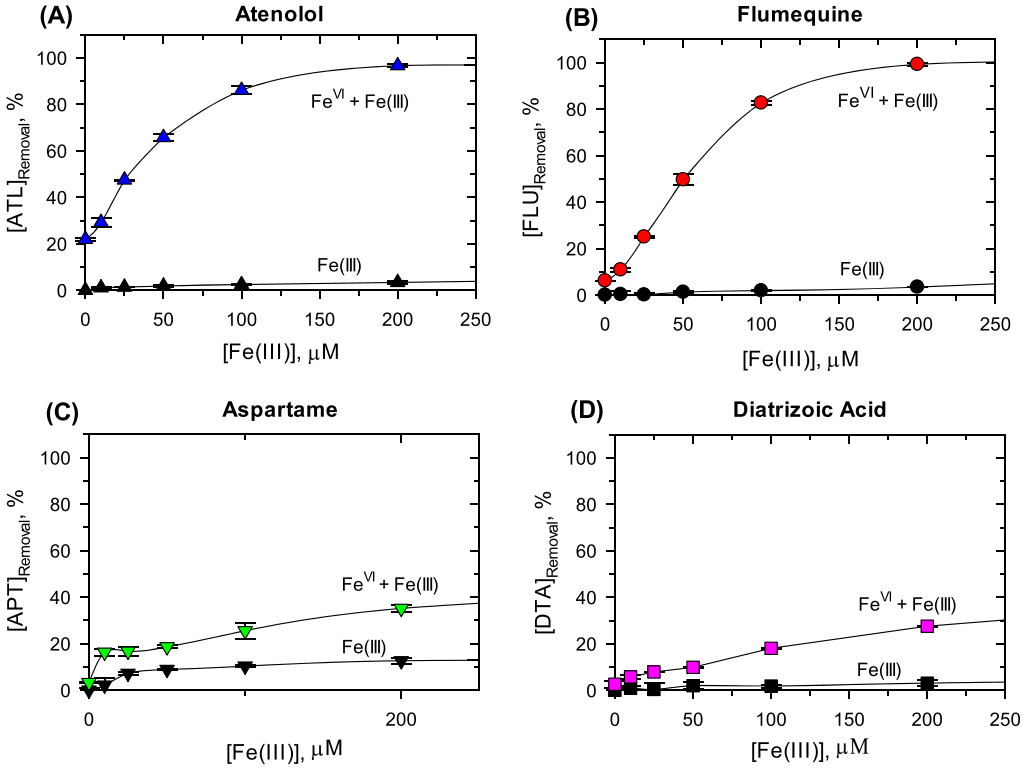

Figure 1. Effect of Fe(III) on removal of ATL, FLU, APT, and DTA by the Fe^{VI}−Fe(III) system. (Experiment conditions: [micropollutant] = 5.0 μM, [Fe(VI)] = 100.0 μM, pH 9.0 ([borate buffer] = 2.0 mM), reaction time = 10 min).

detector. Chromatographic analysis was performed on an ESTEK Ultra C_{18} analytical column (4.6 mm × 250 mm, particle size 5 μm) at 30 °C. The mobile phase was 0.5% H_3PO_4 in ultrapure water and methanol. The other HPLC information for each micropollutant is provided in Table S1. The identification of the OPs of ATL (5.0 μM) by Fe^{VI} (100.0 μM) with and without Fe(III) at pH 9.0 was performed using the solid-phase extraction-liquid chromatography−high-resolution mass spectrometry technique. The detailed operations are described in our recent paper.[16]

Kinetic Modeling. Based on the proposed reactions (discussed later), Simbiology Version 5.7, a kinetic simulation package in MATLAB 2018 (The MathWorks, Inc.), was utilized to estimate the reaction rate constants via the nonlinear least-square regression method. Initially, the "Scan" task was applied to estimate the ranges of k for the reactions. The values of k were subsequently predicted, and standard errors were refined by using the "Fit Data" task through the least-square nonlinear regression with the constant error model. The confidence level and termination tolerance level on estimated coefficients were set to be default (95% and 1×10^{-8}) with maximum iterations to be 1000.

■ RESULTS AND DISCUSSION

Effect of Fe(III). Initially, we have tested the hypothesis that the addition of Fe(III) to the mixture of Fe^{VI}−micropollutant lowers the solution pH, possibly causing the enhanced oxidation of the target pollutant. As shown in Figure S1, adding small amounts of Fe(III) (0−12.0 μM) into Fe^{VI} solution without buffer (i.e., only in water) lowered the pH from 7.0 to 4.5. This suggests that the possibility of the pH lowering effect leads to an increase in the oxidation of the pollutant and that there is a possibility that the observed enhanced effect may not be related to Fe(III) chemistry in the mixture of the Fe^{VI}−micropollutant. To address this potential interference, we explored the specific role of Fe(III) by carrying out the experiments using 2.0 mM borate buffer, which maintained the pH at 9.0 with an increase in concentrations of Fe(III) in the mixed solutions of Fe^{VI}−pollutants. Results showed increased removal of pollutants with Fe(III) additions at pH 9.0 (i.e., without effects of lowering of pH) (Figure 1). This indicated the role of Fe(III) in enhancing the oxidation of pollutants by Fe^{VI}.

Of the four tested pollutants, ATL and FLU showed complete removal (≈100%) with increasing Fe(III) dosages (Figure 1a,b), while APT and DTA had maximum removal up to 35% (Figure 1c,d). Comparatively, no significant removal of pollutants was observed in the exclusive presence of Fe(III) (i.e., without any Fe^{VI}). It appears that the molar ratio of ≈2.0 ([Fe(III)]/[Fe^{VI}]) was sufficient to obtain the maximum removal of the pollutants by the Fe^{VI}−Fe(III) system. Furthermore, a molar ratio of Fe(III) to Fe^{VI} has a critical role in determining the enhancing effect of added Fe(III) to the mixture of the Fe^{VI}−pollutant. A study that showed no effect of Fe(III) to oxidize DCF by Fe^{VI} may be related to the use of the much lower molar ratios of Fe(III) to Fe^{VI} (i.e., 0.02−0.10) in the experiments.[29] Results of Figure 1 indicate that the oxidizing species generated from Fe^{VI} by Fe(III) are largely responsible for enhancing the removal of pollutants. These oxidizing species may be the intermediate Fe^{V}/Fe^{IV} species, produced from the decay of Fe^{VI}, which may be catalyzed by Fe(III) at pH 9.0. These intermediate species are much more reactive than Fe^{VI}. This is in agreement with recent results on the oxidation of SMX by the Fe^{VI}−Fe(III) system in borate buffer.[13] More will be discussed later in the kinetic

https://dx.doi.org/10.1021/acs.est.0c04674
Environ. Sci. Technol. 2021, 55, 623−633

modeling interpretation of the enhanced effect of Fe(III) on the oxidation of pollutants by Fe^{VI}.

The results of Figure 1 indicated that the magnitude of the enhanced effect of Fe(III) depended on the type of pollutant. An attempt was made to understand this trend by determining the second-order rate constants of the reaction between Fe^{VI} and pollutants that initially formed the Fe^{V}/Fe^{IV} species. The obtained rate constants between Fe^{VI} and ATL, FLU, APT, and DTA in 2.0 mM borate buffer at pH 9.0 were $(5.0 \pm 0.4) \times 10^{-1}$, $(3.4 \pm 0.1) \times 10^{-1}$, $(8.2 \pm 1.0) \times 10^{-1}$, and $(5.3 \pm 0.1) \times 10^{-1}$ M^{-1} s^{-1}, respectively. The order of reactivity of Fe^{VI} with the pollutants differed from the trend of removal, as seen in Figure 1, indicating that the nature and reactivity of Fe^{V}/Fe^{IV} species, produced in the Fe^{VI}−Fe(III)−pollutant system, varied with the structure of the pollutant to result in different removal efficiencies by the Fe^{VI}−Fe(III) system.[12] Furthermore, the competitive reactions including self-decomposition of Fe^{V}/Fe^{IV} and the reactions of Fe^{V}/Fe^{IV} with pollutants would determine the overall trend of removal of target compound by the Fe^{VI}−Fe(III) system.

Effect of Fe(III)−TAML. In this study, we also tested the possible role of Fe^{IV}−TAML/Fe^{V}−TAML that may be generated from the reaction of Fe^{VI} and Fe(III)−TAML. The reaction between Fe^{III}−TAML and H_2O_2 in alkaline medium has shown the production of high-valent iron species, complexed with the TAML ligand, to cause the rapid removal of pollutants.[42,45] In our investigation, we first mixed Fe^{VI} with ATL at pH 9.0 in borate buffer, followed by fast addition of Fe^{III}−TAML. The color of Fe^{VI} instantaneously disappeared. The observed results at a varied amount of Fe^{III}−TAML in mixed solutions are presented in Figure 2A. No enhanced effect on the removal of ATL because of the addition of Fe^{III}−TAML to Fe^{VI}−ATL mixture was seen. At higher concentrations of Fe(III)−TAML, the removal of ATL was lower than when there was no addition of Fe(III)−TAML (Figure 2A). It seems that Fe^{VI} reacted with Fe^{III}−TAML or only TAML, but neither of the reaction resulted in the desired oxidizing species necessary to remove ATL. The results of Figure 2A indicated no role of high-valent intermediate species under our experimental conditions.

Effect of Other Metal Ions. Initially, the effect of Ca(II) on the removal of ATL by Fe^{VI} was explored. The results of the effects of increasing amounts of Ca(II), up to 2000 μM, are shown in Figure 2B. The presence of Ca(II) increased the decay of Fe^{VI};[56] however, no enhancement in ATL removal was observed. It appears that the possible Fe^{V}/Fe^{IV} species in the system of Fe^{VI}−ATL−Ca(II) are unable to contribute to the oxidation of ATL. There is a possibility that Ca(II) also destabilizes the Fe^{V}/Fe^{IV} species (or increases their self-decays), thereby minimizing their oxidation reaction time with ATL. This is supported by the known instability of the calcium salt of Fe^{VI} ($CaFeO_4$) in the presence of Fe(III).[46] Similar to Ca(II), Al(III) and Sc(III) have no enhancement effect in the removal of ATL by Fe^{VI} (Figure 2C).

Next, the effect of Co(II) on the removal of ATL by Fe^{VI} was tested (Figure 2C). Co(II) has shown an increase in the decay of Fe^{VI}[36] and could produce the intermediate Fe^{V}/Fe^{IV} species to potentially enhance the removal of ATL. However, the results showed no enhancement by Co(II), similar to Al(III) and Sc(III) under the same conditions. Comparatively, Ni(II) showed enhanced removal of ATL by Fe^{VI} (Figure 2C), although Ni(II) has shown high influence to destabilize the Fe^{VI} even in trace amounts in solution.[36] This suggested that

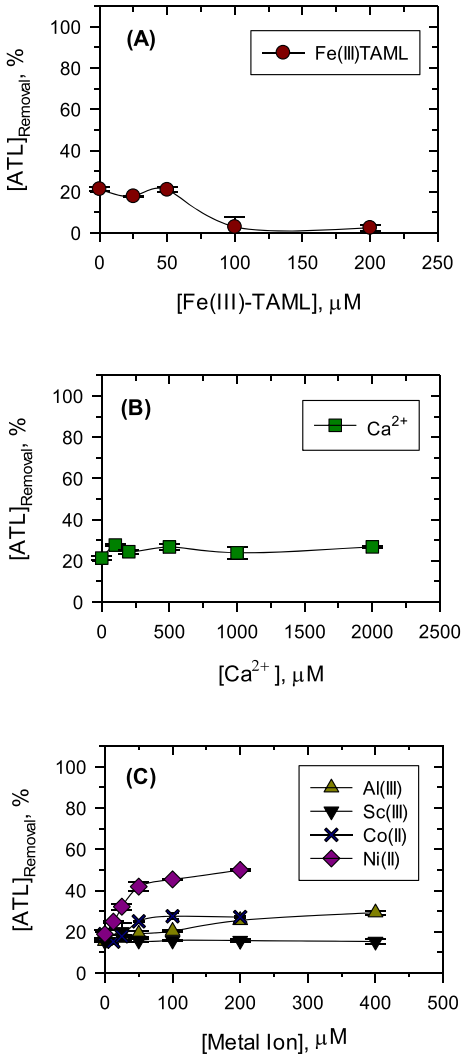

Figure 2. Effect of Fe(III)−TAML and metal ions on degradation of ATL at pH 9.0. (A) Fe(III)−TAML, (B) Ca^{2+} ions, (C) Al(III), Sc(III), Co(II), and Ni(II). (Experiments conditions: [ATL] = 5.0 μM, [Fe(VI)] = 100.0 μM, [borate buffer] = 2.0 mM, and reaction time = 10 min).

the influence of different metal ions on enhancing pollutant removal is largely determined by the competing rate constants of the self-decay of Fe^{V}/Fe^{IV} in the presence of metal ions and the reaction of Fe^{V}/Fe^{IV} with the pollutant.

In further studies of the mechanism and products by the Fe^{VI}−metal ion system, we focused on the Fe(III)-enhanced oxidation of ATL by Fe^{VI}. The Fe^{VI}−Fe(III) system is relatively cleaner and nontoxic[47] and presents a real possibility for use in remediating pollutants in water.

Mechanisms. Initially, the role of Fe^{V}/Fe^{IV} species in the oxidation of pollutants by the Fe^{VI}−Fe(III) system was investigated by oxidizing PMSO as a probing compound. High-valent iron species could selectively oxidize PMSO to $PMSO_2$.[13,25] Fe^{IV}/Fe^{V} species have a much higher reactivity with pollutants than Fe^{VI} does,[48,49] and therefore, the comparative formation rate of $PMSO_2$ would demonstrate the formation of Fe^{IV}/Fe^{V} species in the Fe^{VI}−Fe(III) system. In our experiments, the Fe^{VI} solutions were first mixed with PMSO, followed by the addition of Fe(III) at varying concentrations. The formation of $PMSO_2$ was seen in 10 min. The conversion of PMSO to $PMSO_2$ was ≈10% by Fe^{VI}

https://dx.doi.org/10.1021/acs.est.0c04674
Environ. Sci. Technol. 2021, 55, 623−633

only. However, this conversion increased when Fe(III) was added into Fe^{VI} and became stoichiometric (Figure S2). This suggested that Fe^{V}/Fe^{IV} species were responsible for enhancing the removal of pollutants by the Fe^{VI}−Fe(III) system (see Figure 1).

A direct evidence of the formation of Fe^{IV}/Fe^{V} species in the oxidation of pollutants by Fe^{VI} under our experimental conditions was not possible because the formed Fe^{IV}/Fe^{V} species were short-lived with half-lives ranging from <1 ms to μs and would also be in low amounts.[50,51] The use of stopped-flow kinetic trace experiments to characterize Fe^{IV}/Fe^{V} species spectroscopically[49] is unsuccessful. This is not surprising because the literature available on the Fe^{IV}/Fe^{V}−organic complexes under nonaqueous acetonitrile environment suggested their high instability and could be studied only at below freezing temperatures (e.g., −40 °C).[52,53] Low concentrations of these steady-state high-valent iron intermediates suggested that conventional Mossbauer spectroscopic techniques,[54] commonly used to identify iron species, will not be appropriate. Overall, the technique to identify directly Fe^{IV}/Fe^{V} species in the Fe^{VI}−micropollutant systems under aqueous solutions remains elusive. However, the investigation of decomposition of solid Fe^{VI} using Mossbauer spectroscopy has shown Fe^{IV} as the intermediate species.[37,55] We have therefore applied a kinetic modeling approach to assess which of the two species, that is, Fe^{V} and Fe^{IV}, caused the enhancement.

Kinetic Modeling. The experimental data on the degradation kinetics of ATL by the Fe^{VI}−Fe(III) system were collected at different concentrations of Fe(III) at pH 9.0 to facilitate developing a kinetic model. The results, as shown in Figure 3, were interpreted using the reactions in Table 1.[50,51,56−61] Reactions 1−10 represent the self-decay of Fe^{VI} by water under alkaline conditions.[62] These reactions involve Fe^{V}/Fe^{IV} species and describe the unimolecular decay of Fe^{VI} at pH 9.0 successfully in our previous study.[62] In the presence of Fe(III), additional reaction with Fe(III) occurs and may be one of the six possible reactions 11a−11f. Equation 11a is the reaction between Fe^{VI} and Fe(III) ion to give Fe^{IV} species. In reaction 11a, it is assumed that the added Fe(III) ion behaves the same as the Fe(III) generated in situ from the Fe^{VI} reduction (i.e., self-decay of Fe^{VI} by water), and Fe^{VI} is proposed to react with the total amount of these two types of Fe(III). Equations 11b−11f are the reactions between Fe^{VI} and the added Fe(III) ion only [i.e., the Fe^{VI} reacts much more slowly with Fe(III) formed from Fe^{VI} self-decomposition]. Equations 11b and 11c are the proposed reactions between Fe^{VI} and Fe(III) to generate monomeric Fe^{IV} ($Fe^{IV}O_3^{2-}$) and dimerized Fe^{IV} ($Fe_2^{IV}O_6^{4-}$) species, respectively. Equation 11d represents the proposed reaction between Fe^{VI} and Fe(III) ions to produce Fe^{V}. The subsequent reaction of Fe^{V} with Fe(III) would also generate Fe^{IV} (eq 11e). The reaction of Fe^{VI} with Fe(III) may also form equal proportions of Fe^{V} and Fe^{IV} at the same time (eq 11f). The results of the decay of Fe^{VI}, as shown in Figure S3, were fitted by applying all reactions from 1 to 10 plus one of the possibilities for reaction 11 in the kinetic modelling.

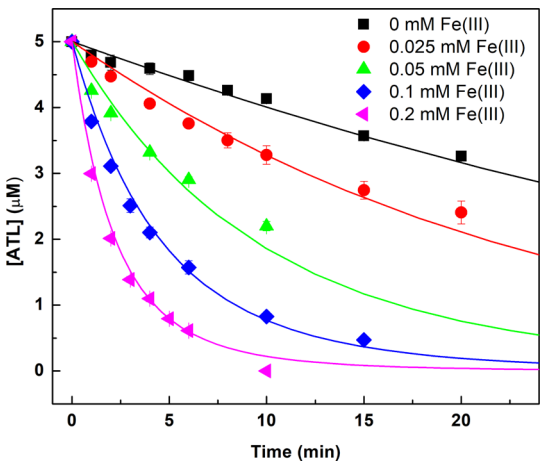

Figure 3. Removal of ATL by the Fe(VI)/Fe(III) system at pH 9.0. (Experimental conditions: [ATL] = 5.0 μM, [Fe(VI)] = 100.0 μM, [borate buffer] = 2.0 mM, and n = 2). Solid lines represent the kinetic modeling.

Of the six possible scenarios (i.e., eqs 11a−f), the best fit of the experimental data in Figure S3 was seen using eq 11b (solid lines of Figures S3 and S4). This indicated that in the Fe^{VI}−Fe(III) system, Fe^{VI} reacted primarily with the added Fe(III) that generated monomeric Fe^{IV} species. This is consistent with a previously reported study on the enhanced decay of Fe^{VI} by freshly added Fe(III) ion.[31] The obtained rate constant for reaction 11b (k_{11b}) from the kinetic modelling was $(2.7 \pm 0.9) \times 10^4$ M^{-2} s^{-1}, which could successfully simulate the Fe^{VI} self-decay at different levels of Fe(III) in the Fe^{VI}−Fe(III) system. The kinetic modeling also revealed that the reaction rate constant between Fe^{VI} and the generated Fe(III) from self-decay of Fe^{VI} by water must be lower than 1×10^2 M^{-2} s^{-1} in order to conform with the observed Fe^{VI} decay and H_2O_2 generation (Figure S5). This further confirms that Fe^{VI} is inherently more reactive toward the added Fe(III) ion compared to produced Fe(III) from the reaction of Fe^{VI} with H_2O. In other words, the reaction of Fe^{VI} with in situ Fe(III) is not significant in the Fe^{VI}−Fe(III) system.

The kinetic modeling of the results demonstrated that the oxidant species to cause enhancement is most likely Fe^{IV} species, which is produced from the reaction of added Fe(III) with Fe^{VI}. Significantly, the evolution profile of the other possible oxidant species, Fe^{V}, in the Fe^{VI}−Fe(III) system was found to be 2 orders of magnitude lower in concentration compared to that of Fe^{IV} species (see Figure S6). This again supported that Fe^{V} was a less important oxidant to promote the degradation of substrates in the Fe^{VI}−Fe(III) system, unless Fe^{V} reactivity toward the substrate was at least 2 orders of magnitude higher than its Fe^{IV} counterpart. Currently, the reactivity trend of Fe^{IV} and Fe^{V} is scarce in the literature and is limited to cyanide at pH ≥ 10.5 only.[63,64]

Finally, reactions of Fe^{VI} and Fe^{IV} with ATL (reactions 12 and 13) were added into the kinetic model (Table 1) to predict the results of Figure 3. In the kinetic simulations, the derived k_{12} and k_{13} values could successfully predict the degradation of ATL at varied concentrations of Fe(III) (see the solid lines of Figures 3 and S7). The strong agreement between the model and multiple sets of experimental data supports the reactions used in modeling the Fe^{VI}−Fe(III)−ATL system to be plausible and that Fe^{IV} is the oxidative species to cause the enhanced oxidation of ATL. Additional support could also be seen in the estimated rate constant for the reaction between Fe^{IV} and ATL ($k(Fe^{IV} + ATL)$) as $(6.3 \pm 0.2) \times 10^4$ M^{-1} s^{-1}, which is much higher than the rate constant for the oxidation of ATL by Fe^{VI} ($k(Fe^{VI} + ATL) = (5.0 \pm 0.4) \times 10^{-1}$ M^{-1} s^{-1}) (Table 1). The derived rate

https://dx.doi.org/10.1021/acs.est.0c04674
Environ. Sci. Technol. 2021, 55, 623−633

Table 1. Possible Reactions in the Fe^{VI}−Fe(III)−ATL System at pH 9.0[a]

reactions	k at pH 9.0	references
[1] $Fe^{VI}O_4^{2-} + H_2O \rightarrow Fe^{IV}O_3^{2-} + H_2O_2$	$(2.0 \pm 0.1) \times 10^{-5}\ s^{-1}$	estimated in the Fe(VI) decay system
[2] $Fe^{VI}O_4^{2-} + H_2O_2 \rightarrow Fe^{IV}O_3^{2-} + O_2 + H_2O$	$\sim 0\ M^{-1}\ s^{-1}$	56
[3] $Fe^{IV}O_3^{2-} + Fe^{IV}O_3^{2-} \rightarrow Fe_2^{IV}O_6^{4-}$	$\sim 10^7\ M^{-1}\ s^{-1}$	51
[4] $Fe_2^{IV}O_6^{4-} + 4H_2O + 4H^+ \rightarrow 2Fe^{III}(OH)_3(H_2O) + H_2O_2$	$10^2\ s^{-1}$	51
[5] $Fe^{IV}O_3^{2-} + H_2O_2 + 2H^+ \rightarrow Fe^{II}(OH)_2(aq) + O_2 + 2H_2O$	$3.0 \times 10^3\ M^{-1}\ s^{-1}$	51,57
[6] $Fe^{IV}O_3^{2-} + Fe^{II}(OH)_2(aq) + 3\ H_2O \rightarrow 2Fe^{III}(OH)_3(aq) + 2OH^-$	$\sim 10^6\ M^{-1}\ s^{-1}$	51
[7] $Fe^{VI}O_4^{2-} + Fe^{II}(OH)_2(aq) + H_2O \rightarrow HFe^{V}O_4^{2-} + Fe^{III}(OH)_3(aq)$	$\sim 10^5\ M^{-1}\ s^{-1}$	58,59
[8] $Fe^{II}(OH)_2(aq) + H_2O_2 + 2OH^- \rightarrow Fe^{IV}O_3^{2-} + 3H_2O$	$\sim 10^3\ M^{-1}\ s^{-1}$	60
[9a] $HFe^{V}O_4^{2-} + 2H^+ + 4H_2O \rightarrow Fe^{III}(OH)_3(H_2O)_3 + H_2O_2$	$5.0\ s^{-1}$	50
[9b] $HFe^{V}O_4^{2-} + HFe^{V}O_4^{2-} + 4H_2O + 4H^+ \rightarrow 2Fe^{III}(OH)_3(H_2O) + 2H_2O_2$	$1.5 \times 10^7\ M^{-1}\ s^{-1}$	61
[10] $HFe^{V}O_4^{2-} + H_2O_2 + H_2O \rightarrow Fe^{III}(OH)_3(aq) + O_2 + 2OH^-$	$4.0 \times 10^5\ M^{-1}\ s^{-1}$	56
[11a] $Fe^{VI}O_4^{2-} + 2Fe^{III}(OH)_3(aq)$ [generated from eqs 1−10 and newly added Fe(III) salts] $+ 4OH^- \rightarrow 3Fe^{IV}O_3^{2-} + 5H_2O$	n.d.	evaluated in the Fe(VI)−Fe(III) system
[11b] $Fe^{VI}O_4^{2-} + 2Fe^{III}(OH)_3$ [newly added Fe(III) salts] $+ 10OH^- \rightarrow 3Fe^{IV}O_3^{2-} + 5H_2O$	$(2.7 \pm 0.9) \times 10^4\ M^{-2}\ s^{-1}$	estimated in the Fe(VI)−Fe(III) system
[11c] $Fe^{VI}O_4^{2-} + 2Fe^{III}(OH)_3(aq)$ [newly added Fe(III) salts] $+ 4OH^- \rightarrow 1.5Fe_2^{IV}O_6^{4-} + 5H_2O$	n.d.	evaluated in the Fe(VI)−Fe(III) system
[11d] $2Fe^{VI}O_4^{2-} + Fe^{III}(OH)_3(aq)$ [newly added Fe(III) salts] $+ 2OH^- \rightarrow 3HFe^{V}O_4^{2-} + H_2O$	n.d.	evaluated in the Fe(VI)−Fe(III) system
[11e] $HFe^{V}O_4^{2-} + Fe^{III}(OH)_3(aq)$ [newly added Fe(III) salts] $+ 2OH^- \rightarrow 2Fe^{IV}O_3^{2-} + 3H_2O$	n.d.	evaluated in the Fe(VI)−Fe(III) system
[11f] $Fe^{VI}O_4^{2-} + Fe^{III}(OH)_3(aq)$ [newly added Fe(III) salts] $+ 2OH^- \rightarrow Fe^{IV}O_3^{2-} + HFe^{V}O_4^{2-} + 2H_2O$	n.d.	evaluated in the Fe(VI)−Fe(III) system
[12] $Fe^{VI}O_4^{2-} + ATL \rightarrow Fe^{III}(OH)_3 + P_1$	$(5.0 \pm 0.4) \times 10^{-1}\ M^{-1}\ s^{-1}$	estimated in the Fe(VI)−Fe(III)−ATL system
[13] $Fe^{IV}O_3^{2-} + ATL \rightarrow Fe^{III}(OH)_3 + P_2$	$(6.3 \pm 0.2) \times 10^4\ M^{-1}\ s^{-1}$	estimated in the Fe(VI)−Fe(III)−ATL system

[a](1) $Fe^{IV}O_3^{2-}$ is the proposed chemical formula of Fe^{IV}, and reactions 3−6 and 8 from the previous studies are modified in this study. (2) The contribution of $HFeO_4^-$ was not shown for simplicity as it only accounted for less than 2% of the concentration of Fe^{VI} at pH 9.0. (3) In eqs. 11b−11f, $Fe^{III}(OH)_3(aq)$ was denoted for the added ferric ions, which are not considered as the same Fe(III) species generated from eqs 1−10 in terms of catalytic capability. (4) n.d. = not determined because of unlikelihood of the reaction.

constant of Fe^{IV} with ATL is consistent with the range of rate constants of the Fe^{IV}−pyrophosphate complex with different inorganic molecules at pH 10.0 reported by an earlier study using the pulse radiolysis stopped flow experiments.[51] Compared to the specialized pulse radiolysis techniques, the kinetic modeling approach of our study provides a simple strategy to estimate the rate constants of Fe^{IV} species with micropollutants in water.

OPs of ATL by Fe^{IV}. In this study, the high-resolution liquid chromatography−mass spectrometry (LC−MS) technique was used for structural identification of OPs of ATL by Fe^{VI} with the addition of Fe(III). The high accuracy of this analytical technique for the determination of m/z values of unknown OPs gives their molecular composition with small mass errors (<1.5 ppm) (Table S2). A total of nine OPs of ATL were identified based on their significantly increased peak areas as compared to the control sample (i.e., ATL without treatment). They are named as OP-282, OP-240, OP-238, OP-224, OP-222, OP-209, OP-193, OP-167, and OP-151, reflective of their approximate m/z value. The detailed information of their MS/MS fragments (Figure S8) facilitated the understanding of the fragmentation patterns of each OP, which provided more structural features. It is noteworthy that some OPs had low MS intensity, and no MS/MS data were therefore available. Together with the reaction pathways of ATL by some other oxidation systems, the molecular structures of all nine OPs of ATL were proposed for the Fe^{VI}−Fe(III) system. Additionally, the OPs of ATL by Fe^{VI} only were also investigated in our study, from which the same OPs were observed, based on the LC−MS analysis.

The possible degradation pathways of ATL by Fe^{VI}−Fe(III) system are presented in Figure 4. As can be noted, two pathways share the following types of oxidative transformations: (1) elimination of the isopropyl group, (2) oxidation of the secondary alcohol, (3) cleavage of the aryl ether, and (4) aromatic and/or benzylic oxidation. Pathway I depicts the first three mentioned transformations, while pathway II is different in that it is preceded by an oxygen addition to ATL, either via aromatic oxidation or benzylic oxidation. Pathway I initiates the oxidative degradation on the secondary amine moiety of ATL, which has been experimentally demonstrated as the reactive site for oxidation.[65] It has been extensively shown that Fe^{IV} is the operative high valence form of iron that can hydroxylate nonactivated C−H bonds, in both heme-type complexes (e.g., cytochrome P450)[66] as well as nonheme iron-based enzymes.[67] While in most of these cases, Fe(II) gets oxidized to Fe(III) in the presence of oxygen gas, followed by the O−O cleavage resulting in subsequent oxidation of Fe(III) to Fe^{IV}; the generation of Fe(IV) in our experiments is a result of the cooperative effect of the Fe^{VI}−Fe(III) combination. Some studies have reflected that the oxidation imposed by Fe^{VI}═O in the hydrogen abstraction of C−H bonds occurs via the diradical character of Fe(III)−O•, also referred to as the oxyl route by which the oxidation is occurring via the oxygen rather than Fe^{IV}.[68] In some regards, the Fe^{IV} in $HFeO_3^-$ receives an electron from the noninnocent oxo ligand, rendering it to be an oxidative radical species. Regardless of which route leads to hydroxylation, the capability of Fe^{IV}═O to initiate a hydrogen abstraction in the hydroxylation, via Fe(III)−OH intermediate,

https://dx.doi.org/10.1021/acs.est.0c04674
Environ. Sci. Technol. 2021, 55, 623−633

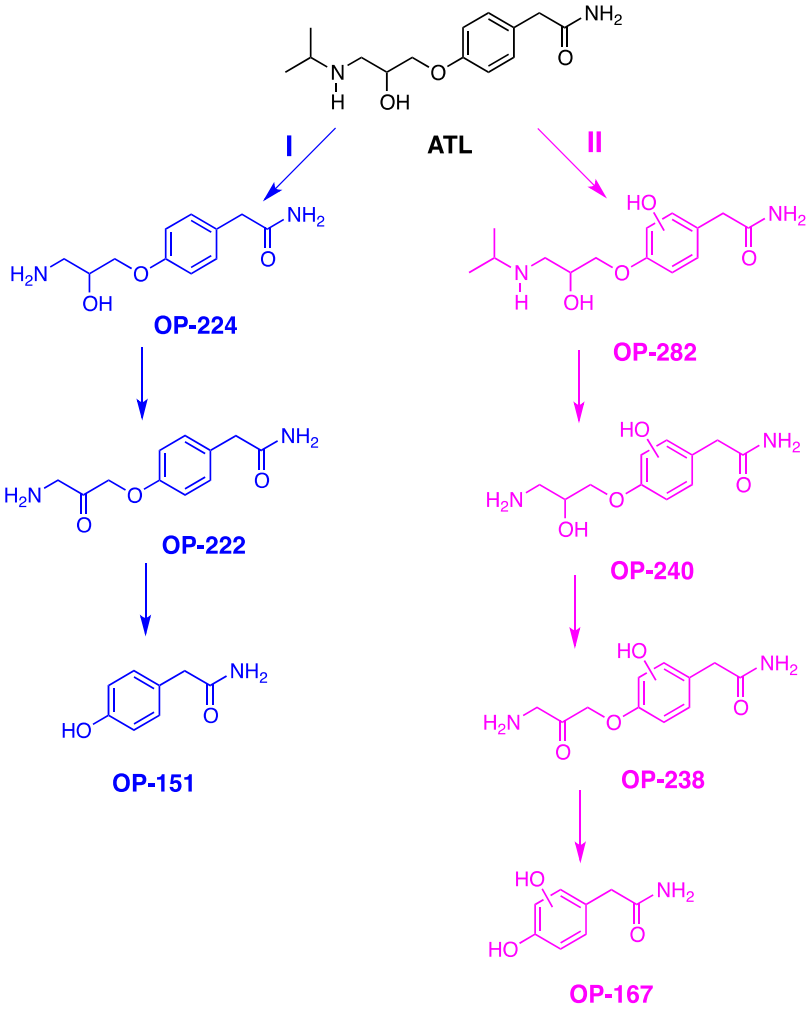

Figure 4. Proposed reaction pathways on the degradation of ATL by the Fe^{VI}−Fe(III) system at pH 9.0. (Experiment conditions: [ATL] = 5.0 μM, [Fe(VI)] = 100.0 μM, [borate buffer] = 2.0 mM, and reaction time = 10 min).

is well studied and generally the accepted mechanism.[69] Enzymatic hydroxylations have the advantage of precise regiocontrol, in part because of their strong binding to their substrate positioning the site of oxidation at proximity to the active site where the iron-oxo of Fe^{IV} resides. Our oxidative pathways do not have such selective regiocontrol, and therefore, the high-valence iron species attacks the most susceptible sites during oxidation.

ATL has four susceptible C−H sites that could lead to stabilized carbon radicals upon hydrogen abstraction by the highly reactive Fe^{IV}═O species. The order of oxidation cannot be easily predicted and may in fact vary as reflected in the two pathways presented in Figure 4. Pathway I shows the abstraction of the secondary C−H of the isopropyl amine group. The detailed mechanism, as shown in Figure 5A, shows an N-stabilized radical, which subsequently receives the local "hydroxyl" radical from Fe(III)−OH leading to the unstable aminoalcohol and an Fe(II) species, which will rapidly oxidize to Fe(III) under the highly oxidative conditions of any of the high valence Fe species (i.e., Fe^{IV}, Fe^{V}, or Fe^{VI}). The aminoalcohol readily loses an acetone molecule, releasing the primary amine OP-224. Subsequent oxidation of the hydroxyl group of OP-224 takes place to form OP-222 initiated by a similar C−H abstraction of the alcohol carbon. The detailed mechanism is shown in Figure 5B, in which the corresponding hydroxylation leads to a gem-diol, which readily loses a water molecule to form OP-222. The cleavage of the phenoxyether evidenced by the observed products in the MS spectrum (Figure S8) occurs via a similar Fe^{IV} C−H abstraction of the α-carbon to both the carbonyl and the phenoxy oxygen. This formed radical (Figure 5C) is stabilized by the carbonyl as well as the oxygen. Subsequent hydroxylation at that position leads to an unstable intermediate that releases the phenol group, OP-151.

Pathway II was initiated by electrophilic attack of Fe^{IV} on the aromatic ring, which can lead to aromatic oxidation, as shown in Figure 5D(a). Similar aromatic oxidations have previously been reported by high-valent metal-oxo species, for example, Fe^{VI},[21] Fe^{V}, and Fe^{IV}.[70] Alternatively and not possible to rule out using MS data, Fe^{IV} could abstract a hydrogen at the benzylic C−H, resulting in the formation of a hydroxylated ATL (having the same mass to the phenolic product, i.e., both OP-282), as shown in Figure 1D(b). The generation of two initial OPs of ATL, that is, OP-224 and OP-282, was also reported during oxidation of ATL by Fe^{VI}.[65] Similar to the transformation patterns of ATL in pathway I, OP-282 was sequentially oxidized leading to the formation of OP-240, OP-238, OP-209, and OP-167.

Environmental Relevance. It is well known that water constituents existing in natural waters could affect the removal

https://dx.doi.org/10.1021/acs.est.0c04674
Environ. Sci. Technol. 2021, 55, 623−633

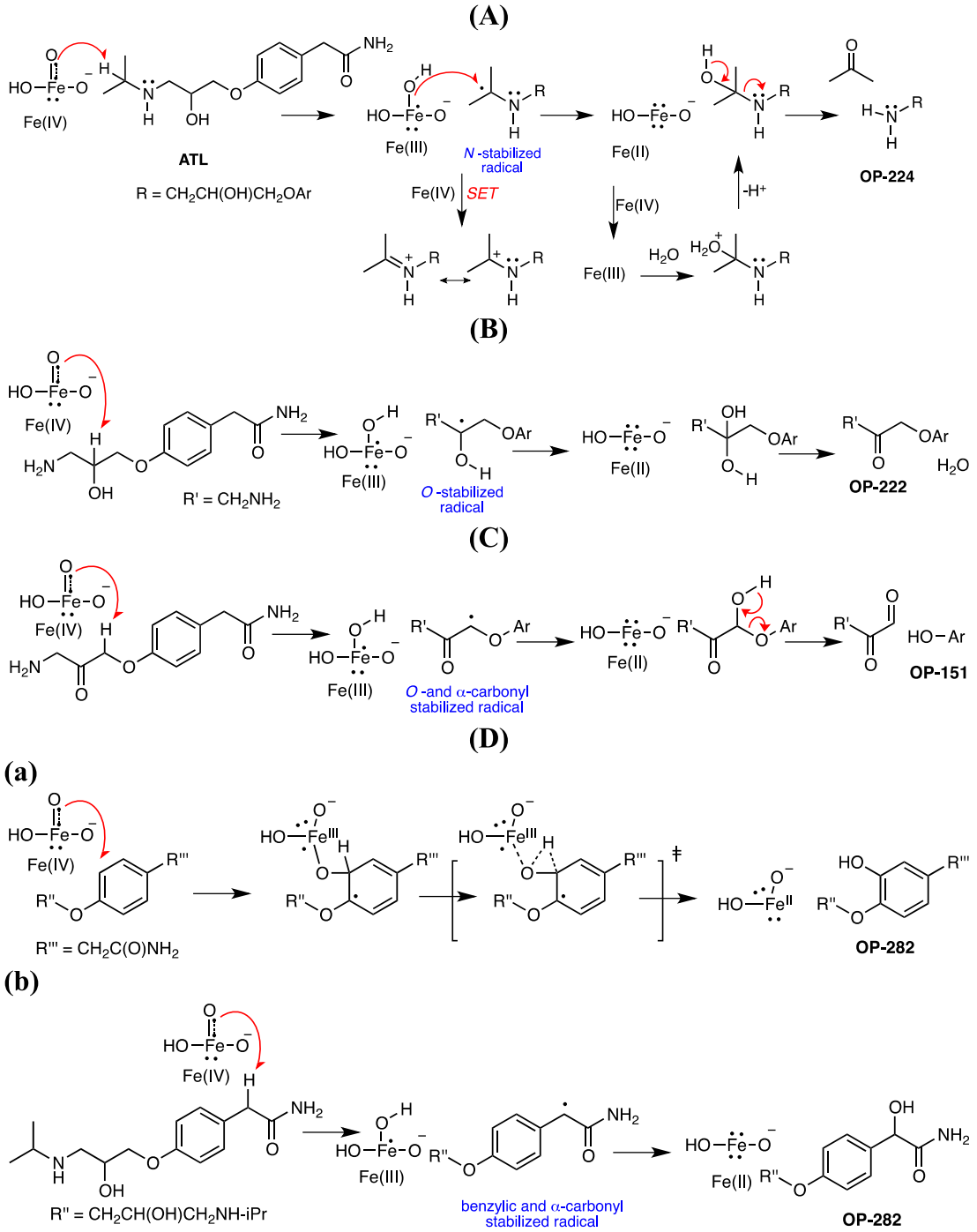

Figure 5. Proposed mechanism by Fe(IV) (A) de-isopropylation of ATL. The lower suggested route is plausible but less probable. The resultant Fe(II) will immediately oxidize back to Fe(III) under the highly oxidative conditions; (B) oxidation of the secondary alcohol via Fe(IV); (C) aryl ether cleavage under Fe(IV); and (D) (a) Fe(IV) electrophilic attack directly on the aromatic ring leading to phenol formation; (b) alternative pathway of benzylic hydroxylation that would lead to oxygen addition to ATL forming an isomer of OP-282 with an identical mass.

efficiency of micropollutants by treatment technologies. In this study, initially, the effect of carbonate and phosphate on the removal of DTA, which is a more recalcitrant pollutant than ATL, was studied independently. When 5.0 mM carbonate was present in solution at pH 9.0, removal of DTA was similar to that without carbonate (16.2 ± 2.2% vs 19.7 ± 1.9%). However, the presence of 5.0 mM phosphate lowered the removal of DTA to 5.5 ± 0.5%. The decrease by phosphate ion agrees with previous studies.[17,29] Next, the effect of SRHA and SRNOM, two representative NOM, was studied for the Fe^{VI}–Fe(III) system. As shown in Figure S9, the significant inhibitory effect of SRHA and SRNOM (5–20 mg/L) on the elimination of all four selected micropollutants (i.e., ATL, FLU, APT, and DTA) by the Fe^{VI}–Fe(III) system was observed following the increased addition of NOM. In the case of ATL and FLU, the decrease in removal was from 100 to ≈20% when the level of NOM and HA increased to 20 mg/L. Under the same conditions, the decrease in removals of APT and DTA was from ≈25 to ≈10%. Generally, no difference in the removal of the micropollutants when adding either

https://dx.doi.org/10.1021/acs.est.0c04674
Environ. Sci. Technol. 2021, 55, 623−633

SRNOM or SRHA was found within experimental errors. It has been documented that the competitive consumption of NOM with reactive oxidizing species (e.g., hydroxyl radicals, sulfate radicals, and Fe^{VI}) greatly diminished the remediation performance of water contaminants.[16,71,72] Similarly, our results may be attributed to the oxidation of NOM by Fe^{IV}, resulting in a lesser amount of Fe^{IV} available for pollutant decomposition.

Finally, the removal of DTA was sought in surface waters (i.e., river water and lake water) by the Fe^{VI}−Fe(III) system (see Figure 1). First, we found that DTA can be completely eliminated at pH 8.0 after 10 min of oxidation by using increasing doses of Fe^{VI} (>200.0 μM) while maintaining the molar ratio of Fe^{VI} to Fe(III) as 0.5 (Figure S10). For the surface waters spiked with 5.0 μM DTA, some higher amounts of Fe^{VI} (i.e., >400.0 μM) and Fe(III) were needed for the complete removal of DTA (Figure S11). In summary, the magnitude of pollutant removal in surface waters will depend on the pH, ions, and the levels and types of NOM. The moieties of pollutants and NOM will also be the factors that influence the degradation of target compounds in water. Some moieties of NOM have acid−base equilibrium (e.g., phenolic),[73] and therefore, the reactivity of NOM with Fe^{VI}/Fe^{IV} would vary with pH. The optimization of solution pH, Fe^{VI} concentration, and molar ratio of Fe^{VI} to Fe(III) may be required to obtain efficient removal of target pollutants in water.

Overall, the findings of our study suggest an important role of Fe(III) to remove micropollutants in water by Fe^{VI} through generation of relatively high amounts of Fe^{IV} species in a short time. The produced amount of Fe^{IV} can be increased proportionally to the addition of Fe(III) into Fe^{VI} in water. In other words, lower Fe^{VI} and higher Fe(III) would give the adequate concentrations of Fe^{IV} species necessary to remove micropollutants rapidly by the Fe^{VI}−Fe(III) system. Because the cost of Fe(III) salts is much less than that of the relatively expensive Fe^{VI} solution, the combination of Fe^{VI} and Fe(III) would make a big stride in the practical use of Fe^{VI} in treatment processes. Furthermore, the applied Fe(III) in treatment plants is in liquid form, which is acidic. Independent studies have shown that small addition of acids also enhanced the oxidation of micropollutants by Fe^{VI} without greatly affecting the pH of the treated water at nearly neutral conditions.[74] This phenomenon would add additional advantages of removing pollutants by the Fe^{VI}−Fe(III) system.

■ ASSOCIATED CONTENT

Supporting Information

The Supporting Information is available free of charge at https://pubs.acs.org/doi/10.1021/acs.est.0c04674.

> Information on the chemicals used and stopped-flow measurements; structures and HPLC conditions of four pollutants and the MS/MS data of ATL and its OPs; pH change by adding Fe(III) without buffering and the PMSO removal by the Fe^{VI}−Fe(III) system, respectively; kinetic modeling results; mass spectra of ATL and its OPs, and removal of pollutants under different conditions (PDF)

■ AUTHOR INFORMATION

Corresponding Authors

Ching-Hua Huang − *School of Civil and Environmental Engineering, Georgia Institute of Technology, Atlanta, Georgia 30332, United States;* orcid.org/0000-0002-3786-094X; Email: ching-hua.huang@ce.gatech.edu

Virender K. Sharma − *Department of Environmental and Occupational Health, School of Public Health, Texas A&M University, College Station, Texas 77843, United States;* orcid.org/0000-0002-5980-8675; Email: vsharma@tamu.edu

Authors

Xianbing Zhang − *Department of Environmental and Occupational Health, School of Public Health, Texas A&M University, College Station, Texas 77843, United States; National Inland Waterway Regulation Engineering Research Center, Chongqing Jiaotong University, Chongqing 400074, China*

Mingbao Feng − *Department of Environmental and Occupational Health, School of Public Health, Texas A&M University, College Station, Texas 77843, United States*

Cong Luo − *School of Civil and Environmental Engineering, Georgia Institute of Technology, Atlanta, Georgia 30332, United States*

Nasri Nesnas − *Department of Biomedical and Chemical Engineering and Sciences, Florida Institute of Technology, Melbourne, Florida 32901, United States;* orcid.org/0000-0003-3511-940X

Complete contact information is available at: https://pubs.acs.org/10.1021/acs.est.0c04674

Author Contributions

⊥X.Z. and M.F. are contributed equally.

Notes

The authors declare no competing financial interest.

■ ACKNOWLEDGMENTS

This study was supported by National Science Foundation grants CBET 1802944 and CBET 1802800.

■ REFERENCES

(1) Yu, X.; Sui, Q.; Lyu, S.; Zhao, W.; Liu, J.; Cai, Z.; Yu, G.; Barcelo, D. Municipal solid waste landfills: An underestimated source of PPCPs in the water environment. *Environ. Sci. Technol.* **2020**, *54*, 9757−9768.

(2) Rasheed, T.; Bilal, M.; Nabeel, F.; Adeel, M.; Iqbal, H. M. N. Environmentally-related contaminants of high concern: Potential sources and analytical modalities for detection, quantification, and treatment. *Environ. Int.* **2019**, *122*, 52−66.

(3) Patel, M.; Kumar, R.; Kishor, K.; Mlsna, T.; Pittman, C. U.; Mohan, D. Pharmaceuticals of emerging concern in aquatic systems: Chemistry, occurrence, effects, and removal methods. *Chem. Rev.* **2019**, *119*, 3510−3673.

(4) Miklos, D. B.; Remy, C.; Jekel, M.; Linden, K. G.; Drewes, J. E.; Hübner, U. Evaluation of advanced oxidation processes for water and wastewater treatment − A critical review. *Water Res.* **2018**, *139*, 118−131.

(5) Monteil, H.; Péchaud, Y.; Oturan, N.; Oturan, M. A. A review on efficiency and cost effectiveness of electro- and bio-electro-Fenton processes: Application to the treatment of pharmaceutical pollutants in water. *Chem. Eng. J.* **2019**, *376*, 119577.

(6) Von Gunten, U. Oxidation Processes in Water Treatment: Are We on Track? *Environ. Sci. Technol.* **2018**, *52*, 5062−5075.

(7) Sharma, V. K.; Feng, M. Water depollution using metal-organic frameworks-catalyzed advanced oxidation processes: A review. *J. Hazard. Mater.* **2019**, *372*, 3−16.
(8) Li, J.; Dou, X.; Qin, H.; Sun, Y.; Yin, D.; Guan, X. Characterization methods of zerovalent iron for water treatment and remediation. *Water Res.* **2019**, *148*, 70−85.
(9) Feng, M.; Wang, Z.; Dionysiou, D. D.; Sharma, V. K. Metal-mediated oxidation of fluoroquinolone antibiotics in water: A review on kinetics, transformation products, and toxicity assessment. *J. Hazard. Mater.* **2018**, *344*, 1136−1154.
(10) Ganiyu, S. O.; Zhou, M.; Martínez-Huitle, C. A. Heterogeneous electro-Fenton and photoelectro-Fenton processes: A critical review of fundamental principles and application for water/wastewater treatment. *Appl. Catal. B Environ.* **2018**, *235*, 103−129.
(11) Sharma, V. K.; Zboril, R.; Varma, R. S. Ferrates: Greener oxidants with multimodal action in water treatment technologies. *Acc. Chem. Res.* **2015**, *48*, 182−191.
(12) Pan, B.; Feng, M.; McDonald, T. J.; Manoli, K.; Wang, C.; Huang, C.-H.; Sharma, V. K. Enhanced ferrate(VI) oxidation of micropollutants in water by carbonaceous materials: Elucidating surface functionality. *Chem. Eng. J.* **2020**, *398*, 125607.
(13) Shao, B.; Dong, H.; Sun, B.; Guan, X. Role of Ferrate(IV) and Ferrate(V) in Activating Ferrate(VI) by Calcium Sulfite for Enhanced Oxidation of Organic Contaminants. *Environ. Sci. Technol.* **2019**, *53*, 894−902.
(14) Shin, J.; Von Gunten, U.; Reckhow, D. A.; Allard, S.; Lee, Y. Reactions of ferrate(VI) with iodide and hypoiodous acid: Kinetics, pathways, and implications for the fate of iodine during water treatment. *Environ. Sci. Technol.* **2018**, *52*, 7458−7467.
(15) Yang, T.; Wang, L.; Liu, Y.; Jiang, J.; Huang, Z.; Pang, S.-Y.; Cheng, H.; Gao, D.; Ma, J. Removal of Organoarsenic with Ferrate and Ferrate Resultant Nanoparticles: Oxidation and Adsorption. *Environ. Sci. Technol.* **2018**, *52*, 13325−13335.
(16) Feng, M.; Wang, X.; Chen, J.; Qu, R.; Sui, Y.; Cizmas, L.; Wang, Z.; Sharma, V. K. Degradation of fluoroquinolone antibiotics by ferrate(VI): Effects of water constituents and oxidized products. *Water Res.* **2016**, *103*, 48−57.
(17) Luo, C.; Feng, M.; Sharma, V. K.; Huang, C.-H. Oxidation of Pharmaceuticals by Ferrate(VI) in Hydrolyzed Urine: Effects of Major Inorganic Constituents. *Environ. Sci. Technol.* **2019**, *53*, 5272−5281.
(18) Karlesa, A.; De Vera, G. A. D.; Dodd, M. C.; Park, J.; Espino, M. P. B.; Lee, Y. Ferrate(VI) oxidation of ß-lactam antibiotics: Reaction kinetics, antibacterial activity changes, and transformation products. *Environ. Sci. Technol.* **2014**, *48*, 10380−10389.
(19) Feng, M.; Baum, J. C.; Nesnas, N.; Lee, Y.; Huang, C.; Sharma, V. K. Oxidation of Sulfonamide Antibiotics of Six-Membered Heterocyclic Moiety byFerrate(VI): Kinetics and Mechanistic Insight into SO_2 Extrusion. *Environ. Sci. Technol.* **2019**, *53*, 2695−2704.
(20) Lee, Y.; Zimmermann, S. G.; Kieu, A. T.; von Gunten, U. Ferrate (Fe(VI)) application for municipal wastewater treatment: A novel process for simultaneous micropollutant oxidation and phosphate removal. *Environ. Sci. Technol.* **2009**, *43*, 3831−3838.
(21) Chen, J.; Xu, X.; Zeng, X.; Feng, M.; Qu, R.; Wang, Z.; Nesnas, N.; Sharma, V. K. Ferrate(VI) oxidation of polychlorinated diphenyl sulfides: Kinetics, degradation, and oxidized products. *Water Res.* **2018**, *143*, 1−9.
(22) Xie, X.; Cheng, H. A simple treatment method for phenylarsenic compounds: Oxidation by ferrate(VI) and simultaneous removal of the arsenate released with *in situ* formed Fe(III) oxide-hydroxide. *Environ. Int.* **2019**, *127*, 730−741.
(23) Sharma, V. K.; Chen, L.; Zboril, R. Review on high valent Fe^{VI} (ferrate): A sustainable green oxidant in organic chemistry and transformation of pharmaceuticals. *ACS Sustainable Chem. Eng.* **2016**, *4*, 18−34.
(24) Feng, M.; Jinadatha, C.; McDonald, T. J.; Sharma, V. K. Accelerated Oxidation of Organic Contaminants by Ferrate(VI): The Overlooked Role of Reducing Additives. *Environ. Sci. Technol.* **2018**, *52*, 11319−11327.
(25) Shao, B.; Dong, H.; Feng, L.; Qiao, J.; Guan, X. Influence of [sulfite]/[Fe(VI)] molar ratio on the active oxidants generation in Fe(VI)/sulfite process. *J. Hazard. Mater.* **2020**, *384*, 121303.
(26) Zhao, J.; Wang, Q.; Fu, Y.; Peng, B.; Zhou, G. Kinetics and mechanism of diclofenac removal using ferrate(VI): roles of Fe^{3+}, Fe^{2+}, and Mn^{2+}. *Environ. Sci. Pollut. Res.* **2018**, *25*, 22998−23008.
(27) Zhao, J.; Liu, Y.; Wang, Q.; Fu, Y.; Lu, X.; Bai, X. The self-catalysis of ferrate(VI) by its reactive byproducts or reductive substances for the degradation of diclofenac: Kinetics, mechanism and transformation products. *Sep. Purif. Technol.* **2018**, *192*, 412−418.
(28) Zheng, L.; Cui, J.; Deng, Y. Emergency Water Treatment with Combined Ferrate(VI) and Ferric Salts for Disasters and Disease Outbreaks. *Environ. Sci. Water Res. Technol.* **2020**, *6*, 2816−2831.
(29) Huang, Z.-S.; Wang, L.; Liu, Y.-L.; Jiang, J.; Xue, M.; Xu, C.-B.; Zhen, Y.-F.; Wang, Y.-C.; Ma, J. Impact of Phosphate on Ferrate Oxidation of Organic Compounds: An Underestimated Oxidant. *Environ. Sci. Technol.* **2018**, *52*, 13897−13907.
(30) Carr, J. D.; Kelter, P. B.; Tabatabai, A.; Spichal, D.; Erickson, L.; McLaughlin, C. W. Properties of ferrate(VI) in aqueous solution: An alternate oxidant in wastewater treatment. *Proceedings of the Conference on Water Chlorination and Chemical Environment Impact Health Effects*, 1985; pp 1285−1298.
(31) Jiang, Y.; Goodwill, J. E.; Tobiason, J. E.; Reckhow, D. A. Effect of different solutes, natural organic matter, and particulate Fe(III) on ferrate(VI) decomposition in aqueous solutions. *Environ. Sci. Technol.* **2015**, *49*, 2841−2848.
(32) Ma, L.; Lam, W. W. Y.; Lo, P.-K.; Lau, K.-C.; Lau, T.-C. Ca^{2+}-Induced Oxygen Generation by FeO_4^{2-} at pH 9-10. *Angew. Chem., Int. Ed.* **2016**, *55*, 3012−3016.
(33) Morimoto, Y.; Kotani, H.; Park, J.; Lee, Y.-M.; Nam, W.; Fukuzumi, S. Metal ion-coupled electron transfer of a nonheme oxoiron(IV) complex: Remarkable enhancement of electron-transfer rates by Sc^{3+}. *J. Am. Chem. Soc.* **2011**, *133*, 403−405.
(34) Park, J.; Morimoto, Y.; Lee, Y.-M.; Nam, W.; Fukuzumi, S. Metal ion effect on the switch of mechanism from direct oxygen transfer to metal ion-coupled electron transfer in the sulfoxidation of thioanisoles by a non-heme iron(IV)-oxo complex. *J. Am. Chem. Soc.* **2011**, *133*, 5236−5239.
(35) Guo, M.; Corona, T.; Ray, K.; Nam, W. Heme and Nonheme High-Valent Iron and Manganese Oxo Cores in Biological and Abiological Oxidation Reactions. *ACS Cent. Sci.* **2019**, *5*, 13−28.
(36) Licht, S.; Wang, B.; Ghosh, S. Energetic iron(VI) chemistry: The super-iron battery. *Science* **1999**, *285*, 1039−1042.
(37) Machala, L.; Sharma, V. K.; Kuzmann, E.; Homonnay, Z.; Filip, J.; Kralchevska, R. P. Thermal decomposition of barium ferrate(VI): Mechanism and formation of Fe^{IV} intermediate and nanocrystalline Fe_2O_3 and ferrite. *J. Alloys Compd.* **2016**, *668*, 73−79.
(38) Machala, L.; Procházka, V.; Miglierini, M.; Sharma, V. K.; Marušák, Z.; Wille, H.-C.; Zbořil, R. Direct evidence of Fe(V) and Fe(IV) intermediates during reduction of Fe(IV) to Fe(III): a nuclear forward scattering of synchrotron radiation approach. *Phys. Chem. Chem. Phys.* **2015**, *17*, 21787−21790.
(39) Delattre, J. L.; Stacy, A. M.; Young, V. G.; Long, G. L.; Hermann, R.; Grandjean, F. Study of the structural, electronic, and magnetic properties of the barium-rich iron(IV) oxides, Ba_2FeO_4 and Ba_3FeO_5. *Inorg. Chem.* **2002**, *41*, 2834−2838.
(40) Herber, R. H.; Johnson, D. Lattice dynamics and hyperfine interactions in M_2FeO_4 (M = K^+, Rb^+, Cs^+) and M'FeO_4 (M' = Sr^{2+}, Ba^{2+}). *Inorg. Chem.* **1979**, *18*, 2786−2790.
(41) Yu, X.; Licht, S. Recent advances in synthesis and analysis of Fe(VI) cathodes: Solution phase and solid-state Fe(VI) syntheses, reversible thin-film Fe(VI) synthesis, coating-stabilized Fe(VI) synthesis, and Fe(VI) analytical methodologies. *J. Solid State Chem.* **2008**, *12*, 1523−1540.
(42) Su, H.; Yu, C.; Zhou, Y.; Gong, L.; Li, Q.; Alvarez, P. J. J.; Long, M. Quantitative structure-activity relationship for the oxidation of aromatic organic contaminants in water by TAML/H_2O_2. *Water Res.* **2018**, *140*, 354−363.

(43) Mills, M. R.; Weitz, A. C.; Hendrich, M. P.; Ryabov, A. D.; Collins, T. J. NaClO-generated iron(IV) oxo ad iron(V)oxo TAML in pure water. *J. Am. Chem. Soc.* **2016**, *138*, 13866−13869.
(44) Sharma, V. K. Potassium ferrate(VI): Environmental friendly oxidant. *Adv. Environ. Res.* **2002**, *6*, 143−156.
(45) Collins, T. J.; Ryabov, A. D. Targeting of High-Valent Iron-TAML Activators at Hydrocarbons and beyond. *Chem. Rev.* **2017**, *117*, 9140−9162.
(46) Xu, Z.; Wang, J.; Shao, H.; Tang, Z.; Zhang, J. Preliminary investigation on the physicochemical properties of calcium ferrate-(VI). *Electrochem. Commun.* **2007**, *9*, 371−377.
(47) Loup, J.; Dhawa, U.; Pesciaioli, F.; Wencel-Delord, J.; Ackermann, L. Enantioselective C-H Activation with Earth-Abundant 3d Transition Metals. *Angew. Chem., Int. Ed.* **2019**, *58*, 12803−12818.
(48) Sharma, V. K. Ferrate(V) oxidation of pollutants: A premix pulse radiolysis. *Radiat. Phys. Chem.* **2002**, *65*, 349−355.
(49) Sharma, V. K. Oxidation of inorganic contaminants by ferrates (Fe(VI), Fe(V), and Fe(IV))- Kinetics and Mechanisms - A Review. *J. Environ. Manage.* **2011**, *92*, 1051−1073.
(50) Rush, J. D.; Bielski, B. H. J. Decay of ferrate(V) in neutral and acidic solutions. A premix pulse radiolysis study. *Inorg. Chem.* **1994**, *33*, 5499−5502.
(51) Melton, J. D.; Bielski, B. H. J. Studies of the kinetics, spectral and chemical properties of Fe(IV) pyrophosphate by pulse radiolysis. *Int. J. Radiat. Appl. Instrum. C Radiat. Phys. Chem.* **1990**, *36*, 725−733.
(52) Lu, X.; Li, X.-X.; Seo, M. S.; Lee, Y.-M.; Clémancey, M.; Maldivi, P.; Latour, J.-M.; Sarangi, R.; Fukuzumi, S.; Nam, W. A Mononuclear Nonheme Iron(IV)-Amido Complex Relevant for the Compound II Chemistry of Cytochrome P450. *J. Am. Chem. Soc.* **2019**, *141*, 80−83.
(53) Hong, S.; Lu, X.; Lee, Y.-M.; Seo, M. S.; Ohta, T.; Ogura, T.; Clémancey, M.; Maldivi, P.; Latour, J.-M.; Sarangi, R.; Nam, W. Achieving One-Electron Oxidation of a Mononuclear Nonheme Iron(V)-Imido Complex. *J. Am. Chem. Soc.* **2017**, *139*, 14372−14375.
(54) Perfiliev, Y. D.; Sharma, V. K. Higher oxidation states of iron in solid state: synthesis and their Mossbauer characterization. *ACS Symp. Ser.* **2008**, *985*, 112−123.
(55) Nowik, I.; Herber, R. H.; Koltypin, M.; Aurbach, D.; Licht, S. Mössbauer spectroscopic studies of the disintegration of hexavalent iron compounds ($BaFeO_4$ and K_2FeO_4). *J. Phys. Chem. Solids* **2005**, *66*, 1307−1313.
(56) Rush, J. D.; Zhao, Z.; Bielski, B. H. J. Reaction of Ferrate(VI)/Ferrate(V) with hydrogen peroxide and superoxide anion- A stopped-flow and premix pulse radiolysis study. *Free Radical Res.* **1996**, *24*, 187−198.
(57) Loegager, T.; Holcman, J.; Sehested, K.; Pedersen, T. Oxidation of ferrous ions by ozone in acidic solutions. *Inorg. Chem.* **1992**, *31*, 3523−3529.
(58) Lee, Y.; Kissner, R.; Von Gunten, U. Reaction of ferrate(VI) with ABTS and self-decay of ferrate(VI): Kinetics and mechanisms. *Environ. Sci. Technol.* **2014**, *48*, 5154−5162.
(59) Sharma, V. K.; Bielski, B. H. J. Reactivity of ferrate(VI) and ferrate(V) with amino acids. *Inorg. Chem.* **1991**, *30*, 4306−4310.
(60) Pestovsky, O.; Bakac, A. Identification and characterization of aqueous ferryl(IV) ion. *Preprints of Extended Abstracts presented at the ACS National Meeting*; American Chemical Society, Division of Environmental Chemistry, 2006; Vol. *46*, pp 573−577.
(61) Rush, J. D.; Bielski, B. H. J. Kinetics of ferrate(V) decay in aqueous solution. A pulse-radiolysis study. *Inorg. Chem.* **1989**, *28*, 3947−3951.
(62) Luo, C.; Feng, M.; Sharma, V. K.; Huang, C.-H. Revelation of ferrate(VI) unimolecular decay under alkaline conditions: Investigation of involvement of Fe(IV) and Fe(V) species. *Chem. Eng. J.* **2020**, *388*, 124134.
(63) Sharma, V. K.; O'Connor, D. B.; Cabelli, D. E. Sequential one-electron reductions of Fe(V) to Fe(III) in alkaline solution. *J. Phys. Chem. B* **2001**, *105*, 11529−11532.
(64) Sharma, V. K. Ferrate(VI) and ferrate(V) oxidation of organic compounds: Kinetics and mechanism. *Coord. Chem. Rev.* **2013**, *257*, 495−510.
(65) Wilde, M. L.; Mahmoud, W. M. M.; Kümmerer, K.; Martins, A. F. Oxidation-coagulation of ß-blockers by $K_2Fe^{VI}O_4$ in hospital wastewater: Assessment of degradation products and biodegradability. *Sci. Total Environ.* **2013**, *452−453*, 137−147.
(66) Hohenberger, J.; Ray, K.; Meyer, K. The biology and chemistry of high-valent iron-oxo and iron-nitrido complexes. *Nat. Commun.* **2012**, *3*, 720.
(67) Krebs, C.; Galonić Fujimori, D.; Walsh, C. T.; Bollinger, J. M., Jr. Non-heme Fe(IV)-oxo intermediates. *Acc. Chem. Res.* **2007**, *40*, 484−492.
(68) Zilberberg, I. L.; Shubin, A. A.; Ruzankin, S. P.; Kovalskii, V. Y.; Ovchinnikov, D. A.; Parmon, V. N. DFT Predictions for Hydrogen Atom Transfer at the $[FeO]^{2+}$ Group: a Distinct Activity of the Oxyl state Fe-III-O-center dot. *Proceedings of the International Conference of Computational Methods in Sciences and Engineering 2016 (ICCMSE-2016)*, 2016; Vol. *1790*; UNSP 020027.
(69) Gani, T. Z. H.; Kulik, H. J. Understanding and Breaking Scaling Relations in Single-Site Catalysis: Methane to Methanol Conversion by Fe^{IV}=O. *ACS Catal.* **2018**, *8*, 975−986.
(70) Ansari, A.; Kaushik, A.; Rajaraman, G. Mechanistic insights on the ortho-hydroxylation of aromatic compounds by non-heme iron complex: A computational case study on the comparative oxidative ability of ferric-hydroperoxo and high-valent Fe^{IV}=O and Fe^{V}=O intermediates. *J. Am. Chem. Soc.* **2013**, *135*, 4235−4249.
(71) Luo, C. W.; Ma, J.; Jiang, J.; Liu, Y. Z.; Song, Y.; Yang, Y.; Guan, Y. H.; Wu, D. J. Simulation and comparative study on the oxidation kinetics of atrazine by UV/H_2O_2, UV/HSO_5^- and UV/$S_2O_8^{2-}$. *Water Res.* **2015**, *80*, 99−108.
(72) Lee, J.; von Gunten, U.; Kim, J.-H. Persulfate-Based Advanced Oxidation: Critical Assessment of Opportunities and Roadblocks. *Environ. Sci. Technol.* **2020**, *54*, 3064−3081.
(73) Önnby, L.; Salhi, E.; Mckay, G.; Rosario-Ortiz, F. L.; von Gunten, U. Ozone and chlorine reactions with dissolved organic matter - Assessment of oxidant-reactive moieties by optical measurements and the electron donating capacities. *Water Res.* **2018**, *144*, 64−75.
(74) Manoli, K.; Morrison, L. M.; Sumarah, M. W.; Nakhla, G.; Ray, A. K.; Sharma, V. K. Pharmaceuticals and pesticides in secondary effluent wastewater: Identification and enhanced removal by acid-activated ferrate(VI). *Water Res.* **2019**, *148*, 272−280.

https://dx.doi.org/10.1021/acs.est.0c04674
Environ. Sci. Technol. 2021, 55, 623−633